Non-contact atomic force microscope: Modeling and simulation using van der Pol averaging method

M. R. Bahrami

Innopolis University, Russia
E-mail: mo.bahrami@innopolis.ru
*Received 27.10.2020, accepted 19.03.2021,
published 31.05.2021*

Abstract. *Topic and aim*. One of the tools which are extremely useful and valuable for creating a topography of surfaces, measuring forces, and manipulating material with nano-meter-scale features is the Atomic force microscope (AFM). Since it can create the image of the surface object in different mediums at the nano-scale, AFM can be used in a wide variety of applications and industries. This work aimed at creating the mathematical model of the non-contact atomic force microscope. *Models and Methods*. The lumped parameter model of the atomic force microscope in the non-contact operation mode is utilized to make the mathematical model of the micro cantilever of the AFM in this article. In this mode, non-contact operation mode, a stiff micro machined cantilever is oscillated by the harmonic external force in the attractive regime, i.e. the sharp tip at the end of the cantilever is quite close to the surface of the specimen but not in contact. In this work, the mathematical model is nonlinear since we use the van der Waals force as the sample-tip interaction. We use the van der Pol average method to find solution of the system and get the frequency response equation. *Results*. This equation was employed to investigate the effect of non-linearity, excitation amplitude, and damping coefficient on the response of the system. Also, the steady-state motion stability was studied, and state space trajectory and timing response of states were demonstrated.

Keywords: Atomic force microscope, AFM, nonlinearity, nonlinear systems, averaging method, non-contact, state response.

Бесконтактный атомно-силовой микроскоп: моделирование и эмуляция с использованием метода усреднения ван дер Поля

М. Р. Бахрами

Университет Иннополис, Россия
E-mail: mo.bahrami@innopolis.ru

Аннотация. *Тема и цель*. Одним из инструментов, чрезвычайно полезным и ценным для создания топографии поверхностей, измерения сил и манипулирования материалом с нанометровыми характеристиками, является атомно-силовой микроскоп (АСМ). Поскольку он может создавать изображение поверхности объекта в различных средах в наноразмерном масштабе, АСМ может использоваться в самых разнообразных приложениях и отраслях промышленности. Данная работа направлена на создание математической модели бесконтактного атомно-силового микроскопа. *Модели и методы*. Для построения математической модели микрокантилевера АСМ в данной статье используется модель сосредоточенных параметров атомно-силового микроскопа в бесконтактном режиме работы. В этом режиме жёсткий микрообработанный кантилевер колеблется под действием гармонической внешней силы в режиме притяжения, то есть острый наконечник на конце кантилевера находится достаточно близко к поверхности образца, но не соприкасается. В этой работе математическая модель нелинейна, так как мы используем силу Ван-дер-Ваальса в качестве взаимодействия образца с наконечником. Мы используем метод усреднения ван дер Поля для нахождения решения системы и получения уравнения частотной характеристики. *Результаты*. Это уравнение было использовано для исследования влияния нелинейности, амплитуды возбуждения и коэффициента затухания на отклик системы. Также была изучена устойчивость стационарного движения, были продемонстрированы траектория пространства состояний и временная реакция состояний.

Ключевые слова: атомно-силовой микроскоп, АСМ, нелинейность, нелинейные системы, метод усреднения, бесконтактный, отклик состояния.

Introduction

Typically, when we want to describe a microscope, we think of it as an optical or electron one. By concentrating electromagnetic radiation on an object surface, these kinds of microscopes make a magnified image of an object where these radiations may be photons and electrons. By using an optical microscope with 1000X magnification and an electron microscope with 100000X magnification, two dimensional magnified images of an object surface can be easily created [1].

Although these microscopes are known as powerful and precise instruments, the images that are obtained by using these instruments are characteristically 2D and located in the horizontal plane of the object surface and the vertical dimensions of the object surface are neglected, i.e. the height and depth of the surface properties, are not taken into account in these microscopes [2–5].

To overcome the drawbacks of the described methods, the atomic force microscope (AFM) invented and developed in the mid-1980s has been used. With an AFM which has a sharp probe, the topography of an object surface can be imaged with enormously high resolutions, up to 1000000X. And on the other hand, one of the most important characteristics of an AFM which makes it a valuable instrument is that the magnification of an AFM is made in three directions, the horizontal *X-Y* plane and the vertical *Z* direction [2–5]. The surface of an object can be imaged with atomic resolution by using an AFM. And also, it was developed to surmount a basic drawback with the STM, scanning tunneling microscope that can just scan conducting or semiconducting surfaces. However, it is an advantage

for the AFM that can image different types of surfaces in different mediums [5–8].

One of the tools which are extremely useful and valuable for creating a topography of surfaces, measuring forces, and manipulating material with nano-meter-scale features is the Atomic force microscope (AFM). Since it may create the image of the surface object in different mediums at the nano-scale, AFM can be used in a wide variety of applications and industries. By probing the surface of the specimen with a micro cantilever, the data required to create a surface image is gathered. Utilizing piezoelectric elements, facilitating small but exact movements on electronic command, capable the AFM to construct the most accurate and precise scanning.
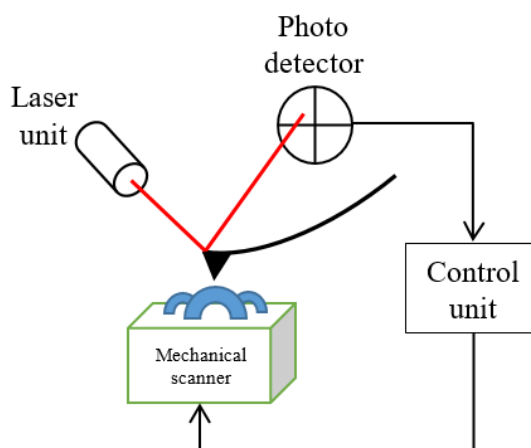

Fig. 1. Typical AFM schematic

Fig. 1 illustrates a conventional AFM system. The AFM comprises a sharp tip located at the end of a micro cantilever installed on a piezoelectric (PZT) actuator and a photo detector which receives a laser spot repulsed from the end-point of the cantilever probe to track the deflection of the micro cantilever for obtaining feedback. The AFM working principle is to probe the surface of the specimen by moving the tip over it with mechanisms that provide feedback and allow the mechanical scanners, PZT, to keep the tip of the cantilever at a constant height over the surface of the sample, i.e. keep the interaction force constant.

Changing the contour of the surface of the specimen the tip is moving up and down when it probes the surface of the sample. As a result of these movements, the laser beam deflects and the difference in light tenseness between the upper and lower photo detectors is calculated. The feedback signal obtained from the photo detector odds passes via the control unit and makes the cantilever tip able to be kept either invariable force or prefixed height (constant height) above the surface of the specimen. In mode, where the force is invariable, real-time height deviation is monitored by the PZT transducer, and in the prefixed height mode, the flexure force on the sample is measured [4].

The AFM is an extremely useful tool for various applications as it is capable of scanning surfaces in a vacuum, air, or in liquids with atomic resolution, manipulating objects with nanometer-scale characteristics, and also measuring forces with better than pico-newton resolution.

Since an AFM is the most powerful instrument for imaging the sample surface and due to its advantages, it has a variety of applications. Applications of an AFM can be classified into three major categories: molecular metrology, biological science, and force spectroscopy [2–5, 7, 8].

The dynamic behavior of the micro cantilever, in various modes of operations, is an interest of many researchers and different methods have been used to accomplish this [6, 9–15]. Here, we used the lumped parameter model of the cantilever to obtain the mathematical model, and then we solved it using the van der Pol averaging method. The influence of non-linearity variable, excitation amplitude, and damping coefficient on the response of the system is studied through the frequency response equation. To study the steady-state stability, the nature of the singular points is investigated.

1. AFM cantilever modeling

The most important component of an AFM which has a high influence on the effective operation and performance of the AFM is the micro-cantilever. Therefore, to improve the efficient operation of the AFM, it is necessary to have a complete analysis of its dynamics. Several models have been presented
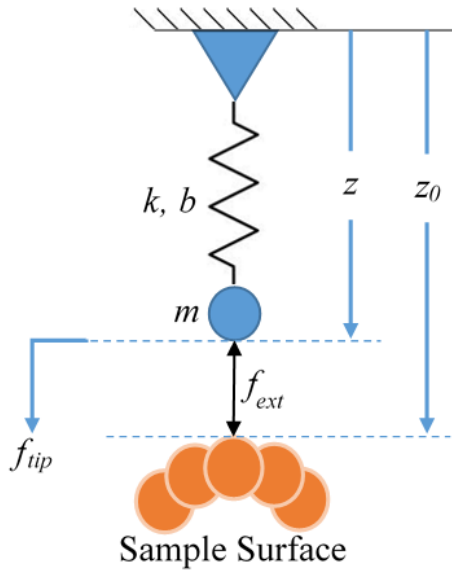
Бахрами М. Р.
Известия вузов. ПНД, 2021, т. 29, № 3

347

Fig. 2. The tip excited AFM cantilever: Lumped-parameter model

to describe the interaction forces between the tip and the surface of the specimen. In this project, the lumped parameter model is employed to create the cantilever model.

Fig. 2 illustrates the lumped model of the cantilever. In this model, the mass of the micro cantilever, m, is located at end the of a massless spring with the stiffness k and damping coefficient b.

We write the equation of motion of the system as:

$$m\frac{\mathrm{d}^2 z}{\mathrm{d}\tau^2} + b\frac{\mathrm{d}}{\mathrm{d}\tau}z + kz = f_{\mathrm{tip}}(z(\tau)) + f_{\mathrm{ext}}(\tau). \quad (1)$$

In non-contact operation mode, a stiff cantilever is oscillated by the harmonic external force, f_{ext}, in the attractive regime, meaning that the tip is quite close to the sample but not touching it. In this work, we consider the sample-tip interaction, $f_{\mathrm{tip}}(z(\tau))$, is the van der Waals sphere-plane force, which makes the model nonlinear [5, 13, 15]. (2) presents these forces:

$$f_{\mathrm{ext}}(\tau) = A_E \cos \omega\tau,$$
$$f_{\mathrm{tip}}(z(\tau)) = \frac{A_H R}{6(z_0 - z)^2}, \quad (2)$$

where A_H is the coefficient of Hamaker, and R is the tip apex radius. It should be noted that the z_0 is the fixed space between the stationary stage and the surface of the object, sample here.

Inserting (2) in (1) we obtain:

$$m\frac{\mathrm{d}^2 z}{\mathrm{d}\tau^2} + b\frac{\mathrm{d}z}{\mathrm{d}\tau} + kz = \frac{A_H R}{6(z_0 - z)^2} + A_E \cos \omega\tau. \quad (3)$$

To find the equilibrium point of the system, in (3) we set all the time terms and the excitation force amplitude to zero as:

$$z_s = \frac{3}{2}(2H)^{\frac{1}{3}},$$
$$H = \frac{A_H R}{6k}. \quad (4)$$

The dimensionless equation of motion can be obtained by setting:

$$x = \frac{z}{z_s}, \quad t = \omega_0\tau, \quad F = \frac{A_E}{z_s}, \quad \zeta = \frac{z_0}{z_s},$$
$$c = \frac{4}{27}, \quad \phi = \frac{\omega}{\omega_0}, \quad B = \frac{b}{m\omega_0}, \quad \omega_0 = \sqrt{k/m}, \quad (5)$$

and inserting in (3) as:

$$\ddot{x} + B\dot{x} + x = \frac{c}{(\zeta - x)^2} + F \cos \phi t. \quad (6)$$

In this paper, derivation with respect to t is designated by dots.

2. Van der Pol averaging method

In our system, since we have a system containing time-scales division, i.e. quickly vibrating terms versus a slow drift, the method of averaging is a good option. The van der Pol averaging method suggests to perform an averaging over the vibration period of time in order to smooth the fast fluctuations and study the resulting dynamics. To employ van der Pol averaging method, first we approximated the van der Waals sample-tip interaction force around the relax point z_s:

$$
\frac{c}{(\zeta - x)^2} = \frac{c}{(\zeta - z_s)^2} + \frac{2c}{(\zeta - z_s)^3}(x - z_s) + \\
+ \frac{3c}{(\zeta - z_s)^4}(x - z_s)^2 + \frac{(n+1)c}{(\zeta - z_s)^{(n+2)}}(x - z_s)^n. \tag{7}
$$

Introducing

$$
\alpha_0 = \frac{c}{(\zeta - z_s)^2}, \quad \alpha_1 = \frac{2c}{(\zeta - z_s)^3}, \quad \alpha_2 = \frac{3c}{(\zeta - z_s)^4}, \quad \ldots \quad \alpha_n = \frac{(n+1)c}{(\zeta - z_s)^{(n+2)}},
$$

and setting $y = x - z_s$, one can rewrite (6) as:

$$
\ddot{y} + \omega_{0n}^2 y = -B\dot{y} + F\cos\phi t + \alpha_0 + \alpha_2 y^2 + \alpha_3 y^3 + \cdots + \alpha_n y_n^n \tag{8}
$$

where $\omega_{0n} = \sqrt{1 - \alpha_1}$.

As mentioned before, in the non-contact mode the frequency of external excitation is close to the natural frequency of the oscillation part, where the frequency disorder $\phi = \omega_{0n} + \delta$ is small. Here, δ is named detuning parameter that presents how close ϕ is to ω_{0n}. As one can notice, the right hand side terms are related to dissipation, non-linearity, and external effects. By ignoring these terms, the system turns into a typical harmonic vibrator. The solution may be found in the quasi-harmonic vibration form with a amplitude that varies slowly since the dissipation, non-linearity, and external are assumed to be small. To accomplish this, using asymptotic methods one can write the simplified equation of (8) in the following form:

$$
y(t) = A(t)\exp\{i\omega_{0n}t\} + \bar{A}(t)\exp\{-i\omega_{0n}t\}. \tag{9}
$$

Also, it should be mentioned that there is an extra condition on the slowly changing complex amplitude A:

$$
\dot{A}(t)\exp\{i\omega_{0n}t\} + \dot{\bar{A}}(t)\exp\{-i\omega_{0n}t\} = 0. \tag{10}
$$

Writing the excitation force as:

$$
F\cos\phi t = \operatorname{Re} F\exp\{i\phi t\} = \frac{F\exp\{i\phi t\} + \bar{F}\exp\{-i\phi t\}}{2}. \tag{11}
$$

It should be noted that in this work, $\bar{\square}$ is the complex conjugate of $\square$.
The first and second derivative of (9) with respect to time t will be presented as:

$$
\dot{y} = i\omega_{0n}A\exp\{i\omega_{0n}t\} - i\omega_{0n}\bar{A}\exp\{-i\omega_{0n}t\}, \\
\ddot{y} = 2i\omega_{0n}\dot{A}\exp\{i\omega_{0n}t\} - \omega_{0n}^2 A\exp\{i\omega_{0n}t\} - \omega_{0n}^2 \bar{A}\exp\{-i\omega_{0n}t\}. \tag{12}
$$

Бахрами М. Р.
Известия вузов. ПНД, 2021, т. 29, № 3

349

Inserting (12) and (9) in (8), we get:

$$2i\omega_{0n}\dot{A}\exp\{i\omega_{0n}t\} = -Bi\omega_{0n}A\exp\{i\omega_{0n}t\} + Bi\omega_{0n}\bar{A}\exp\{-i\omega_{0n}t\} + \frac{1}{2}F\exp\{i\phi t\}+$$

$$+ \frac{1}{2}\bar{F}\exp\{-i\phi t\} + \alpha_0 + \alpha_2 A^2 \exp\{2i\omega_{0n}t\} + 2\alpha_2 A\bar{A} + \alpha_2\bar{A}^2\exp\{-2i\omega_{0n}t\} + \alpha_3\{\ldots\} + \ldots$$

(13)

First we divide both sides of (13) by $i\omega_{0n}A\exp\{i\omega_{0n}t\}$ and then do averaging over the given period of time, here the vibration period, $\frac{2\pi}{\omega_{0n}}$ we get:

$$2\dot{A} = -BA - i\frac{F}{2\omega_{0n}}\exp\{i\delta t\} - \alpha_3\frac{i}{\omega_{0n}}|A|^2 A.$$

(14)

The altering in complex amplitudes can be ignored at this timeline. Also, the term including the exponent will be insensibly varying since in the case that we consider, the frequencies and are close. Therefore, one can write the simplistic equation of (14) by omitting the fast oscillating terms.

The solution of (14) can be presented as:

$$A = a\exp\{i\beta\},$$

(15)

where a and β are real variables.

Inserting (15) into (14), and splitting the real and imaginary parts yields:

$$2\dot{a}\cos\beta - 2a\dot{\beta}\sin\beta = -Ba\cos\beta + \frac{F}{2\omega_{0n}}\sin\delta t + \alpha_3\frac{a^3}{\omega_{0n}}\sin\beta,$$

(16)

$$2\dot{a}\sin\beta + 2a\dot{\beta}\cos\beta = -Ba\sin\beta - \frac{F}{2\omega_{0n}}\cos\delta t - \alpha_3\frac{a^3}{\omega_{0n}}\cos\beta.$$

(17)

Introducing $\psi = \delta t - \beta$ and solving for $\dot{a}$ and $\dot{\beta}$, we obtain:

$$\dot{a} + \frac{1}{2}Ba = \frac{F}{4\omega_{0n}}\cos\psi,$$

$$\dot{\psi} = \delta - \frac{a^2\alpha_3}{2\omega_{0n}} - \frac{F}{4a\omega_{0n}}\sin\psi.$$

(18)

Setting $\dot{a} = \dot{\psi} = 0$ provides:

$$\frac{2Ba\omega_{0n}}{F} = \cos\psi,$$

$$\left(\delta - \frac{a^2\alpha_3}{2\omega_{0n}}\right)\frac{4a\omega_{0n}}{F} = \sin\psi.$$

(19)

To obtain the frequency response equation, we square and add terms in (19):

$$\left[\frac{2Ba\omega_{0n}}{F}\right]^2 + \left[\left(\delta - \frac{a^2\alpha_3}{2\omega_{0n}}\right)\frac{4a\omega_{0n}}{F}\right]^2 = 1.$$

(20)

Now, we can use (20) to examine the influence and effects of the non-linearity, the amplitude of excitation (excitation force), and the coefficient of damping on the response of the system. It should be mentioned again, that the system is excited by an external harmonic force with a frequency near to the natural frequency of the micro cantilever.

(20) presents that the peak of the amplitude, $a_p = F/2\omega_{0n}B$, does not depend on the α_3, the non-linearity. The effect of the non-linearity on the response amplitude is shown in Fig. 3, a.

The excitation amplitude effect is shown in Fig. 3, b. As we expected, the response amplitude increases by increasing the the external force. It should be noted that the frequency-response curves are multi-valued for some values of detuning δ (Fig. 3, b).

Fig. 4, a illustrates the linear and nonlinear plots. As shown in Fig. 4, a, the linear response occurs by setting $\alpha_3 = 0$. It means that when ζ goes to infinity, the linear case happens. The other interesting thing is that the peak amplitude does not depend on the value of α_3, as presented in Fig. 4, a. By changing the sign of α_3 (in the nonlinear cases, when $\alpha_3 \neq 0$) the graph slanting to the right or left.

Fig. 4, b presents the effect of the excitation intensity on the response equation. As one can see, with the higher the amplitude of the excitation force the amplitude of response increases as well.

In Fig. 4, c, the effect of the damping coefficient on the frequency response is presented. As illustrated, the peak of the response amplitude reduces by growing the damping coefficient. The amplitude goes to infinity setting the damping coefficient to zero.

In nonlinear dynamical systems take place phenomena where the oscillation amplitude can harshly grow or reduce as the excitation frequency is increased or decreased and multi-valued areas appeared. The multivaluedness implies that two amplitudes of oscillation exist for a given external frequency. This yields to the phenomena that are famous and known as the jump phenomenon [16] as presented in Fig. 4, d by arrows.

If one from the left-hand side of the plot increases the δ (the excitation frequency) the amplitude grows till reaching point 1 on the graph. As a result of a further increase in δ, a jump happens from point 1 to point 2. From point 2 the amplitude decreases by growing δ. And if we start from the right-hand side and decrease the δ, subsequently the amplitude increase until attaining point 3 on the plot where
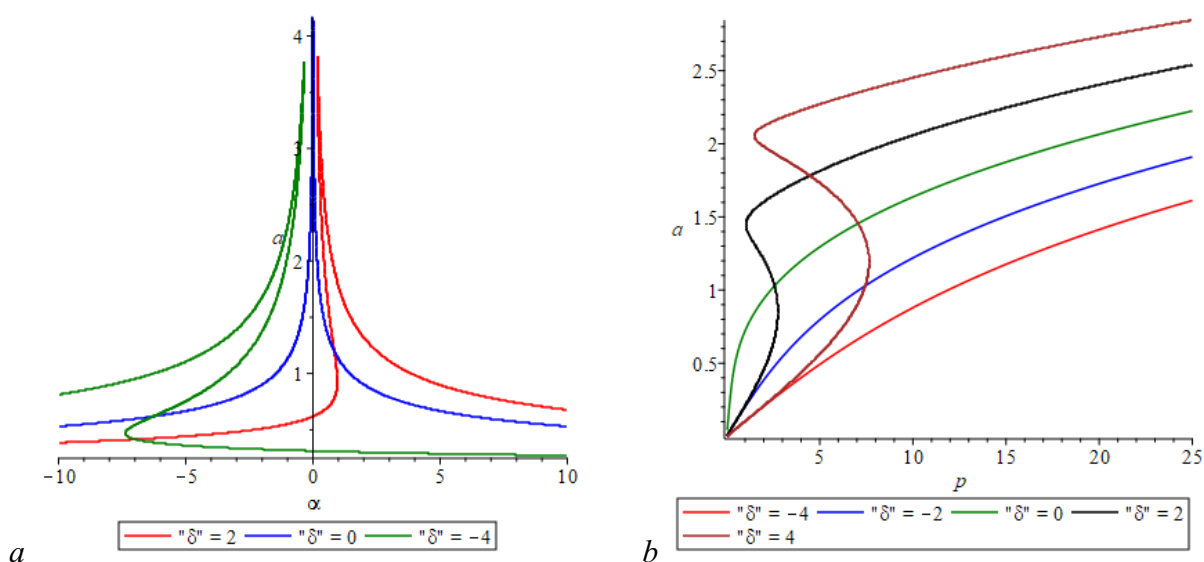

Fig. 3. a – Effect of the non-linearity, b – the excitation amplitude on the response amplitude for several detunings
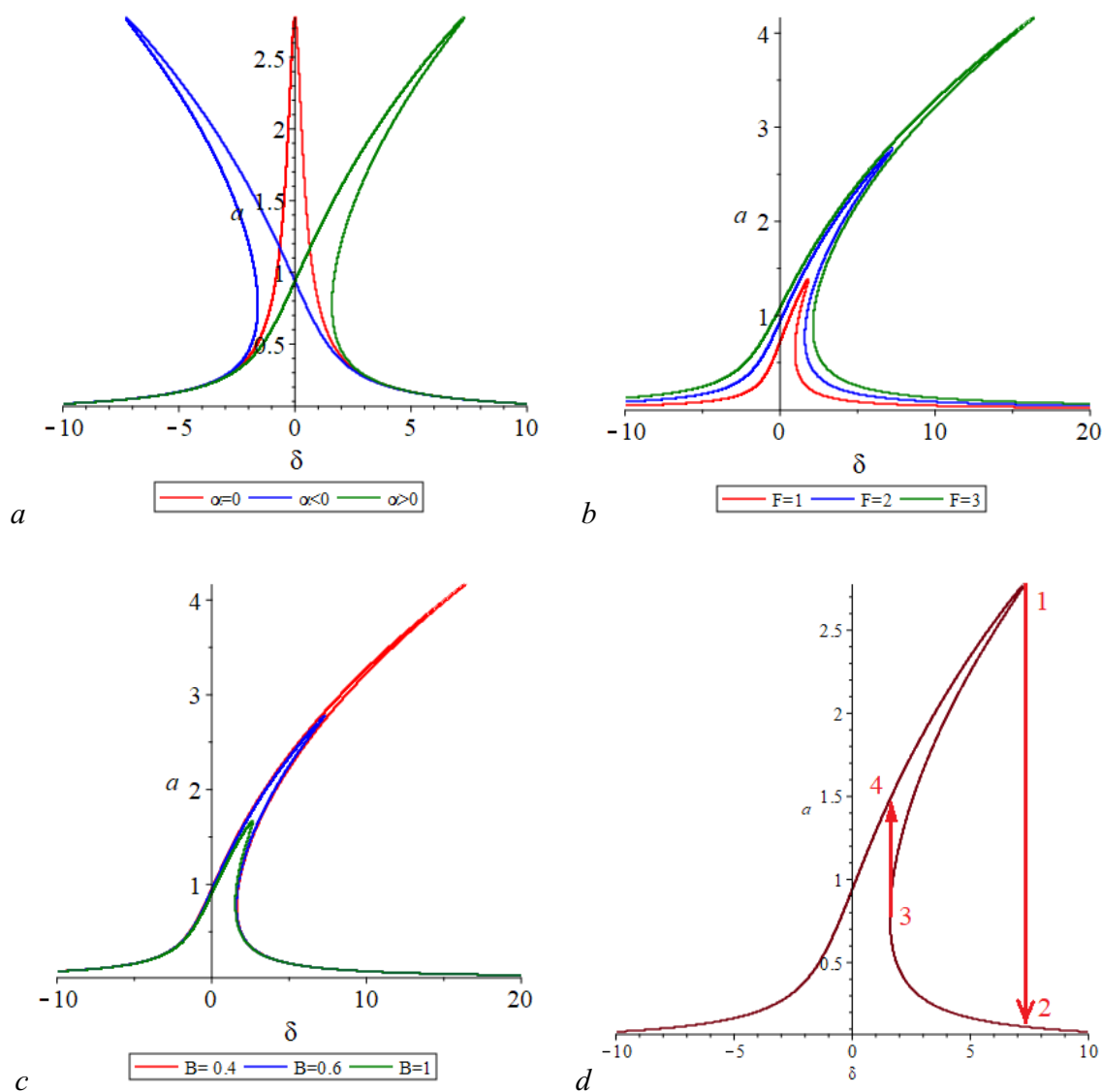
Fig. 4. *a* – Effect of non linearity, *b* – effect of excitation, *c* – effect of damping, *d* – jumping phenomenon

again a jump happens to the upper point (point 4 on the plot). This can be summarized as follow, the amplitude of the response may bounce to the higher amplitude by an increase in the frequency of the external excitation, and by a decrease in the frequency of the excitation, the response amplitude might jump to lower amplitude [16].

3. Stability of the steady-state motions

There exists various methods to investigate the stability of the steady state motions [16–20].

To analysis the steady-state stability, the stability of the various sections of the response graph, by investigating the nature of the singular points of (18), one may set:

$$a = a_0 + a_1,$$
$$\psi = \psi_0 + \psi_1. \tag{21}$$

Inserting (21) into (18), expanding for small a_1 and ψ_1 and removing nonlinear terms in a_1 and ψ_1, we obtain:

$$\dot{a_1} = -\frac{1}{2}B\,a_1 - \left(\frac{F}{4\omega_{0n}}\sin\psi_0\right)\psi_1,$$

$$\dot{\psi_1} = \left(-\frac{a_0\alpha_3}{\omega_{0n}} + \frac{F\sin\psi_0}{4a_0^2\omega_{0n}}\right)a_1 - \left(\frac{F}{4a_0\omega_{0n}}\cos\psi_0\right)\psi_1. \tag{22}$$

It should be noted that a_0 and ψ_0 satisfy (19).

Therefore, stability of the steady state motions depends on the eigenvalues of the coefficient matrix conducted from the right-hand sides of (22). Subsequently, one gets the equation of the eigenvalues through (19):

$$\begin{vmatrix} -\frac{1}{2}B - \lambda & -a_0\left(\frac{3}{2}\frac{a_0^2\alpha_3}{\omega_{0n}} - \delta\right) \\ -\frac{1}{a_0}\left(\frac{a_0^2\alpha_3}{2\omega_{0n}} - \delta\right) & -\frac{1}{2}B - \lambda \end{vmatrix} = 0. \tag{23}$$

Expanding (23) we conclude that the instability of the steady-state motions happens when

$$\frac{1}{4}B^2 + \left(\frac{3}{2}\frac{a_0^2\alpha_3}{\omega_{0n}} - \delta\right)\left(\frac{a_0^2\alpha_3}{2\omega_{0n}} - \delta\right) < 0, \tag{24}$$

and the steady-state motions are otherwise stable.

Fig. 5 demonstrates the State space trajectory and timing response of states with two initial conditions; with the initial $(2, 0, 0)^T$ are shown in Fig. 5, *a* and 5, *b*, while the initial $(-2, 0, 0)^T$ satisfies stabilization conditions, but neither the system is stable.
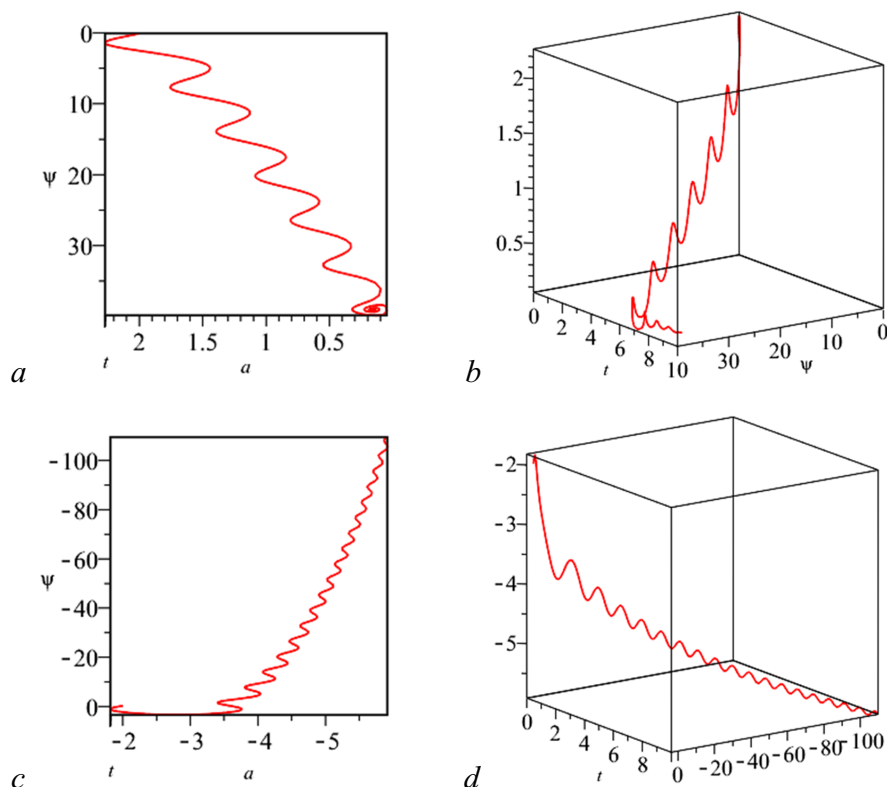

Fig. 5. *a* – State space trajectory and *b* – timing response of states with the initial $(2, 0, 0)^T$, *c* – state space trajectory and *d* – timing response of states with the initial $(-2, 0, 0)^T$

Бахрами М. Р.
Известия вузов. ПНД, 2021, т. 29, № 3

353

Conclusion

The typical AFM contains a probe installed at the end of a micro cantilever that is utilized to scan the surface of the specimen and is used for gaining resolution in the scale of atomic. The micro machined cantilever usually is a beam from materials; silicon or silicon nitride. At the end of this beam is installed a sharp tip with the radius on the order of nanometers. When this sharp tip extends toward a surface of a specimen, in concordance with Hooke's law, the micro cantilever, because of the sample-tip interaction force, deflects. To monitor the cantilever deflection a laser unit is employed. An array of photodiodes is employed to gather the reflected laser spot from the top surface of the cantilever. Then, a mechanism that provides feedback to adjust the sample-tip distance (to keep the interaction force constant) is used. Typically, a mechanical scanner consists of a piezoelectric tube that is utilized for holding the specimen and used to accomplish the goal which is to keep the interaction force constant. This PZT tube moves the sample in the x - y plane as well as in the z direction. By mapping the area, the scan of the surface of the sample is created [21].

This work aimed at creating the mathematical model of the non-contact atomic force microscope. To accomplish this, the lumped parameter model is utilized. In non-contact operation mode, a stiff cantilever is oscillated by the harmonic external force in the attractive regime, i.e. the sharp tip at the end of the cantilever is quite close to the surface of the specimen but not in contact. Here, we used the van der Waals force as the sample-tip interaction force. This sample-tip interaction force makes the model nonlinear. The van der Pol method was utilized to solve the system and find the frequency response equation. It followed by, investigating the effect of non-linearity, excitation amplitude, and damping coefficient on the response of the system utilizing the frequency response equation. The stability of steady-state motion was explored using the nature of the singular points and state space trajectory and timing response of states has been illustrated.

References

1. Binnig G, Quate CF, Gerber C. Atomic force microscope. Physical Review Letters. 1986;56(9): 930–933. DOI: 10.1103/PhysRevLett.56.930.

2. Seo Y, Jhe W. Atomic force microscopy and spectroscopy. Reports on Progress in Physics. 2007;71(1):016101. DOI: 10.1088/0034-4885/71/1/016101.

3. Marrese M, Guarino V, Ambrosio L. Atomic force microscopy: A powerful tool to address scaffold design in tissue engineering. Journal of Functional Biomaterials. 2017;8(1):7. DOI: 10.3390/jfb8010007.

4. Liu S, Wang Y. Application of AFM in microbiology: A review. Scanning. 2010;32(2):61–73. DOI: 10.1002/sca.20173.

5. Jalili N, Laxminarayana K. A review of atomic force microscopy imaging systems: application to molecular metrology and biological sciences. Mechatronics. 2004;14(8):907–945. DOI: 10.1016/j.mechatronics.2004.04.005.

6. Bahrami M, Ramezani A, Osquie KG. Modeling and simulation of non-contact atomic force microscope. ASME 2010 10th Biennial Conference on Engineering Systems Design and Analysis. ESDA, 12-14 July 2010, Istanbul, Turkey. Vol. 5. P. 565–569. DOI: 10.1115/ESDA2010-24394.

7. Dufrêne YF, Ando T, Garcia R, Alsteens D, Martinez-Martin D, Engel A, Gerber C, Müller DJ. Imaging modes of atomic force microscopy for application in molecular and cell biology. Nature Nanotechnology. 2017;12(4):295–307. DOI: 10.1038/nnano.2017.45.

8. Gautsch S. Development of an Atomic Force Microscope and Measurement Concepts for Characterizing Marian Dust and Soil Particles. PhD thesis. Universite de Neuchatel; 2002. 133 p.

9. Bahrami MR, Abeygunawardana AWB. Modeling and simulation of tapping mode atomic force

microscope through a bond-graph. Advances in Mechanical Engineering. Springer, Cham; 2018. P. 9–15. DOI: 10.1007/978-3-319-72929-9_2.

10. Bahrami MR, Abeygunawardana AWB. Modeling and simulation of dynamic contact atomic force microscope. Advances in Mechanical Engineering. Springer, Cham; 2019. P. 109–118. DOI: 10.1007/978-3-030-11981-2_10.

11. Sebastian A, Salapaka MV, Chen DJ, Cleveland JP. Harmonic analysis based modeling of tapping-mode AFM. Proceedings of the 1999 American Control Conference. AAC, 2-4 June 1999, San Diego, CA, USA. Vol 1. P. 232–236. DOI: 10.1109/ACC.1999.782775.

12. Belikov S, Magonov S. Classification of dynamic atomic force microscopy control modes based on asymptotic nonlinear mechanics. 2009 American Control Conference. AAC, 10-12 June 2009, St. Louis, MO, USA. P. 979–984. DOI: 10.1109/ACC.2009.5160048.

13. Couturier G, Boisgard R, Nony L, Aimé JP. Noncontact atomic force microscopy: Stability criterion and dynamical responses of the shift of frequency and damping signal. Review of Scientific Instruments. 2003;74(5):2726–2734. DOI: 10.1063/1.1564274.

14. Bahrami MR. Dynamic analysis of atomic force microscope in tapping mode. Vibroengineering PROCEDIA. 2020;32:13–19. DOI: 10.21595/vp.2020.21488.

15. Bahrami MR, Suvorov V. Virtual non-contact atomic force microscope. IOP Conference Series: Materials Science and Engineering. Quality Management and Reliability of Technical Systems, 20-21 June 2019, St Petersburg, Russian Federation. Vol. 666. P. 012008.
DOI: 10.1088/1757-899X/666/1/012008.

16. Nayfeh AH, Mook DT. Nonlinear Oscillations. John Wiley and Sons; 1995. 720 p.

17. Eliseev VV, Bahrami MR. A diagnostic machine on power transmission lines: Configuration and mechanical challenges. St. Petersburg State Polytechnic University Journal. 2015;214(1):200–208 (in Russian). DOI: 10.5862/JEST.214.23.

18. Weaver Jr W, Timoshenko SP, Young DH. Vibration Problems in Engineering. 5th Edition. John Wiley and Sons; 1990. 624 p.

19. Eliseev VV, Bahrami MR. Dynamic of electrical transmission wires at a diagnostic machine movement along the line. Journal of Instrument Engineering. 2015;58(3):229–235 (in Russian). DOI: 10.17586/0021-3454-2015-58-3-229-235.

20. Eliseev VV, Bahrami MR. Dynamic of electrical transmission lines with inspection robot on it under influence of limited power of robot engine. Theory of Mechanisms and Machines. 2015;13(4):6–11 (in Russian). DOI: 10.5862/TMM.28.1.

21. Eaton P, West P. Atomic Force Microscopy. Oxford University Press; 2010. 248 p.
DOI: 10.1093/acprof:oso/9780199570454.001.0001.

Мохаммад Реза Бахрами получил степень бакалавра в области машиностроения Университета Шахида Бахонар-и-Керман (Иран, 2005), степень магистра в области мехатроники в Технологическом университете Шарифа, Международный кампус, остров Киш (Иран, 2010) и докторскую степень и диплом инженера-механика Санкт-Петербургского политехнического университета Петра Великого (Россия, 2016). Награжден грантом за работу преподавателем вуза по программе 5-100 Санкт-Петербургского политехнического университета Петра Великого (в 2016, 2017 и 2018 годах) и грантом на соискание ученой степени доктора философии студентов программы 5-100 Санкт-Петербургского политехнического университета Петра Великого (в 2014 и 2015 годах). Автор более 50 научных работ, в том числе двух книг, одна из которых на русском языке.

Россия, 420500 Иннополис, ул. Университетская, 1
Университет Иннополис
E-mail: mo.bahrami@innopolis.ru
ORCID: 0000-0003-4050-701X